Spatial beam self-cleaning dynamics in Erbium-Ytterbium (Er-Yb) codoped multimode fiber

A. Niang[1], F. Mangini[1], D. Modotto[1], A. Tonello[2], U. Minoni[1], M. Fabert[2], V. Couderc[2] and S. Wabnitz[3]

[1]*Dipartimento di Ingegneria dell'Informazione, Università di Brescia, via Branze 38, 25123, Brescia, Italy*
[2]*Université de Limoges, XLIM, UMR CNRS 7252, 123 Avenue A. Thomas, 87060 Limoges, France*
[3]*DIET, Sapienza University of Rome, Via Eudossiana 18, 00184 Rome, Italy*

alioune.niang@unibs.it

Abstract: We demonstrate self-induced high beam quality recovery in Er-Yb codoped multimode active fiber with parabolic refractive index profile of the core. Nonlinear beam cleanup is accompanied by Raman and parametric instability sideband generation.

Graded-index (GRIN) multimode fibers (MMFs) have become essential tools in the study of spatiotemporal and spectral dynamics of optical waves. These fibers exhibit a periodic self-imaging effect, leading to a periodic refractive index modulation induced by Kerr nonlinearity, and have low modal dispersion, which permits fiber modes to have long interaction lengths. Multimode optical solitons [1], geometrical parametric instabilities (GPI) [2], modulation instability [3], Kerr beam-self-cleaning [4], ultra-wide supercontinuum generation [5, 6], and intermodal four-wave mixing (IFWM) [7, 8] can be cited among the major experimental advances. Nonlinear propagation has been investigated in both the normal and anomalous dispersion regime, by using standard GRIN MMFs, including passive [9] and active [10] multimode tapers.

Here we demonstrate the possibility of generating, via Kerr self-cleaning, a high quality beam in a specially designed Erbium-Ytterbium codoped (EYD) MMF with a parabolic index profile. Our experimental results in a passive configuration (i.e., without any pump laser diode) confirm the self-cleaning of a highly multimode beam, leading to record improved beam quality ($M^2 = 1.5$), accompanied by spectral broadening and different nonlinear frequency conversion processes.

The specially designed Erbium-Ytterbium codoped (EYD) GRIN MMF fiber, with uniform doping distribution in the core cross-section, mass concentration of 1.4 % for Yb and 0.6 % for Er, has a core diameter of 65 μm and square cladding with 200 μm side. In order to study nonlinear beam dynamics in a 3 m long EYD GRIN MMF, we used an input Gaussian beam at 1064 nm, with a pulse duration of 500 ps and a repetition rate of 500 Hz. We used a polarizing beam-splitter and two half-wave plates for adjusting peak power and polarization state of the input beam, which was focused into the Er-Yb MMF with a beam diameter of 14 μm at full width of half maximum intensity (FWHMI). The output beam was imaged with a micro-lens on a CCD camera and on the input of an optical spectrum analyzer, to monitor spatial and spectral distributions, respectively.

First, by increasing the input coupled peak power (P_{in}) from 0.7 kW up to 56 kW (maximum input peak power), we characterized the output spatial intensity distributions as a function of the power injected into the EYD MMF. Different transverse modes were excited: for low values of input coupled peak power, the spatial output beam pattern was speckled. Increasing of the input peak power leads to a self-organization of the output transverse intensity distribution, leading to spatial beam cleanup above P_{in}=5 kW, that we attribute to Kerr self-cleaning. The insets of Fig. 1a summarize these observations.

Next, we studied the power dependence of the output spectrum profile (see Fig. 1b). The output spectral distribution remained almost unchanged as a function of input peak power, well above the appearance of self-cleaning. With an input peak power around 20 kW, large pedestals appear around 1064 nm and 1550 nm (red curve in Fig. 1b). The pedestal close to 1064 nm comes from self-phase modulation, while that around 1550 nm can be related to energy transfer from Yb ions toward Er ions. The intensity of both pedestals increases with input peak power, until stimulated Raman scattering (SRS) leads to a Stokes peak at 1116 nm (corresponding to a -13.4 THz shift) for P_{in}=24 kW (blue curve). Moreover, for P_{in}=29 kW we observed two sidebands at 1041 nm and 1088 nm (green curve), corresponding to a ±6.4 THz shift. The presence of these two sidebands may be attributed to IFWM. At the input peak power of 37 kW, we observed an anti-Stokes sideband at 1016 nm (magenta curve). By gradually increasing the input peak power, significant spectral broadening around 1064 nm and towards longer wavelengths can be observed. Finally, from P_{in}=52.6 kW to P_{in}=56 kW we observed the generation of two additional spectral peaks in the visible region: 739 nm (124 THz) and 624 nm (199 THz). These sidebands have a frequency shift of

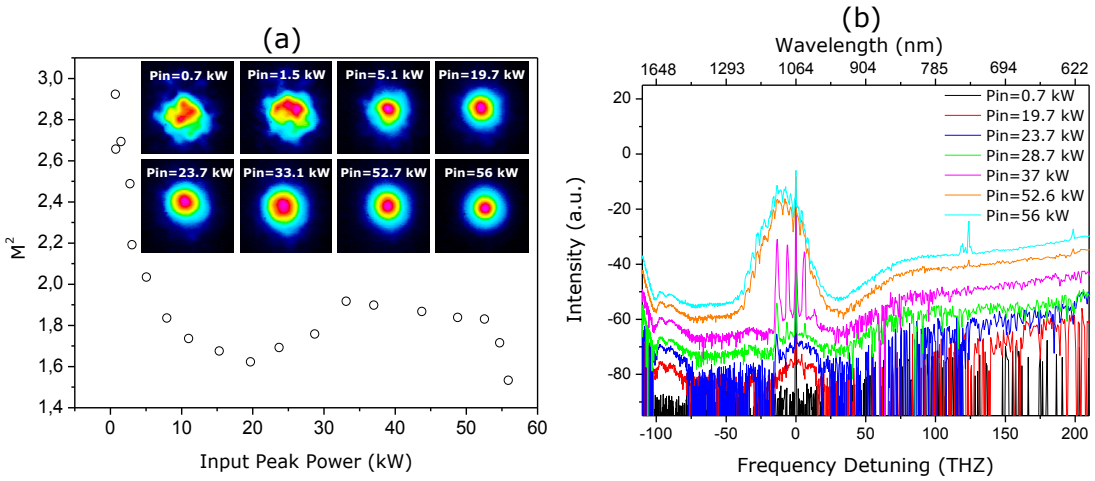

Fig. 1. a) Beam quality M^2 parameter vs. input peak power, inset near-field spatial intensity distributions, (b) spectra as function of input peak power.

more than 100 THz from the input laser, which can be due to GPI [2, 3]. By using bandpass filter at 740 nm (10 nm bandwidth), we observed a bell-shaped beam for an input peak power of 56 kW.

We analytically calculated the frequency position of GPI sidebands, by using the relation $f_h \approx \pm\sqrt{h} f_m$ with h=1,2,3, ... and $f_m = (\sqrt{2\pi/(\Lambda\kappa'')})/2\pi$, where $\Lambda = \pi R/\sqrt{2\Delta}$ (R: fiber core radius and Δ: relative index difference) and κ'' are the self-imaging period and the group velocity dispersion (GVD), respectively. According to Ref. [10], we used the GVD coefficient $\kappa'' = 16.55 \times 10^{-27} s^2/m$ at 1064 nm for a standard GRIN MMFs [3]. The calculated frequency detuning of the first and second anti-Stokes GPI sidebands are f_1=123 THz and f_2=174 THz respectively. These theoretical predictions are in good agreement with experiments for the first-order GPI sideband, but a discrepancy with the second-order one is observed.

Finally, we measured the near-field and far-field output beam diameters, in order to verify the beam quality at the EYD GRIN MMF output. For this purpose, we calculated the input power dependence of the beam quality factor M^2 of the output beam (along its two orthogonal transverse directions). Fig. 1a presents the beam quality M^2 parameter versus input peak power. As can be seen, the beam quality is strongly improved as the input peak power grows above the self-cleaning threshold: the M^2 factor drops from 3 to 1.5. Note that the M^2 parameter increases slightly from P_{in}=24 kW to P_{in}=33 kW. This increase is visible in the insets of Fig. 1a, and it is due to beam depletion by SRS (see Fig. 1b), which degrades beam quality at the input beam wavelength.

We demonstrated highly effective spatial beam cleaning in a EYD GRIN MMF in a passive configuration: a beam quality factor M^2=1.5 was obtained, a record low value for Kerr-cleaning experiments to date. As perspective for further work, by adding a pump laser diode our nonlinear active fiber will permit us the generation of an ultra-broadband continuum, as well as nonlinear beam cleaning and amplification in the telecom window at 1550 nm.

We thank O.N. Egorova, A.E. Levchenko, and S.L. Semjonov from the Fiber Optics Research Center of the Russian Academy of Sciences (RAS), and D.S. Lipatov from the Devyatykh Institute of Chemistry of High-Purity Substances of RAS, for providing the EYD GRIN MMF. We acknowledge the financial support from the European Research Council (grant No. 740355) and the Italian Ministry of Education, University and Research (MIUR) under PRIN 2015 NEMO project (grant No. 2015KEZNYM).

References

1. W.H. Renninger, et al., Nat. Commun. 4, 1719 (2013).
2. K. Krupa, et al., Phys. Rev. Lett. 116, 183901 (2016).
3. S. Longhi, Opt. Lett. 28, 2363–2365 (2003).
4. K. Krupa, et al., Nat. Photonics, 11, 237-241 (2017).
5. G. Lopez-Galmiche, et al. Opt. Lett. 41, 2553–2556 (2016).
6. K. Krupa, et al. Opt. Lett. 41, 5785–5788 (2016).
7. E. Nazemosadat, et al., J. Opt. Soc. Am. B 33, 144–150 (2016).
8. A. Bendahmane, et al., J. Opt. Soc. Am. B 35, 295–301 (2018).
9. M. A. Eftekhar, et al., Nat Commun, 10, 1638 (2019).
10. A. Niang, et al., Opt. Express, 27, 24 018–24 028 (2019).